ORIGINAL PAPER



Proton affinity studies of nickel N₂S₂ complexes and control of aggregation

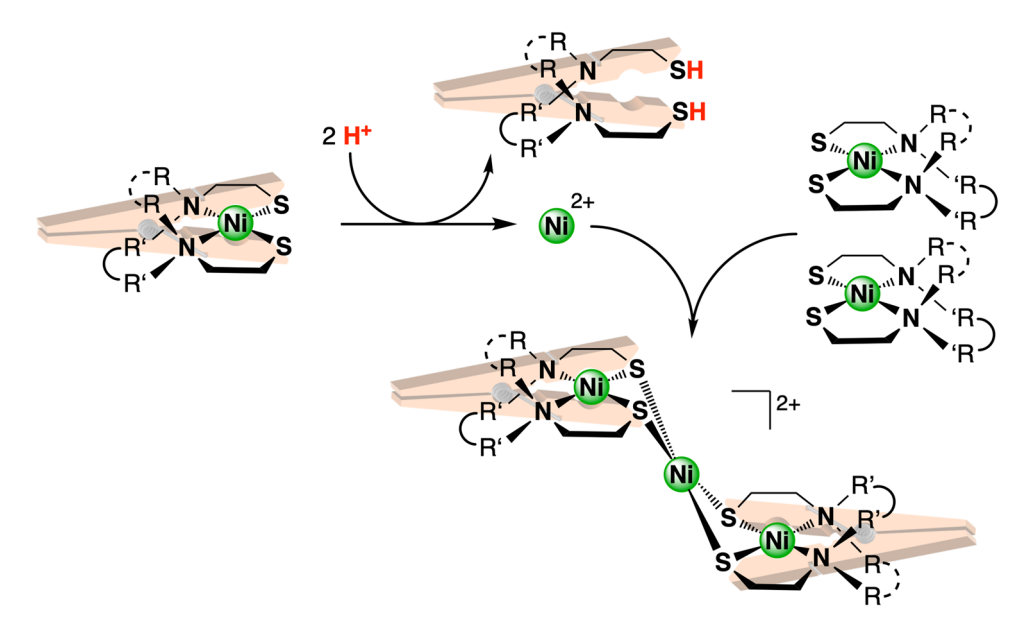
Nicholas A. Arnet¹ · Nattamai Bhuvanesh¹ · Marcetta Y. Darensbourg¹

Received: 1 April 2019 / Accepted: 22 May 2019 © Society for Biological Inorganic Chemistry (SBIC) 2019

Abstract

The thiolate ligands of [NiFe]-H₂ase enzymes have been implicated as proton-binding sites for the reduction/oxidation of H⁺/H₂. This study examines the ligand effect on reactivity of NiN₂S₂ complexes with an array of acids in methanol solution. UV–Vis absorption spectroscopy is utilized to observe the transformation from the monomeric species to a trimetallic complex that is formed after proton-induced ligand dissociation. Nickel complexes with a flexible (propyl and ethyl) N to N linker were found to readily form the trimetallic complex with acids as weak as ammonium (pK_a = 10.9 in methanol). A more constrained nickel complex with a diazacycloheptane N to N linker required stronger acids such as 2,2-dichloroacetic acid (pK_a = 6.38 in methanol) to form the trimetallic complex and featured the formation of an NiN₂S₂H⁺ complex with acetic acid (pK_a = 9.63 in methanol). The most strained ligand, which featured a diazacyclohexane backbone, readily dissociated from the nickel center upon mixture with acids with pK_a ≤ 9.63 and showed no evidence of a trimetallic species with any acid. This research highlights the dramatic differences in reactivity with proton sources that can be imparted by minor alterations to ligand geometry and strain.

Graphical abstract



Electronic supplementary material The online version of this article (https://doi.org/10.1007/s00775-019-01671-4) contains supplementary material, which is available to authorized users.

Extended author information available on the last page of the article

Published online: 07 June 2019



Introduction

From multiple experimental directions, the past two decades have seen tremendous advances in the characterization of hydrogenase enzymes [1, 2]. Such research has highlighted the evolutionarily perfected routes to deliver electrons and protons to the active sites of the metalloenzymes as well as the reverse of H₂ oxidation with recovery of reductive power. The diiron hydrogenase, [FeFe]-H₂ase, active site utilizes a strategically placed amine base, an azadithiolate (adt), to facilitate catalytic turnover. The nitrogen of this adt ligand is aptly described as a pendant base, positioning protons in the optimal location to be transferred to and reduced by the adjacent iron sites as electron sources to ultimately form H₂. The amine serves as the final proton holding site prior to H⁺/H⁻ coupling and H₂ formation. Many synthetic proton reduction catalysts have been designed to have an amine pendant base within a metallo-azacycle, with a notable positive effect on catalytic performance [2].

In contrast to the [FeFe]- H_2 ase active site (Fig. 1a), the likely pendant base within the [NiFe]- H_2 ase (Fig. 1b) is a cysteinyl sulfur, held in position on the unusual distorted Ni(SCys)₄ of the heterobimetallic active site. An impressive high-resolution crystal structure finds a heterolytically split H_2 , with proton on a terminal thiolate and a hydride

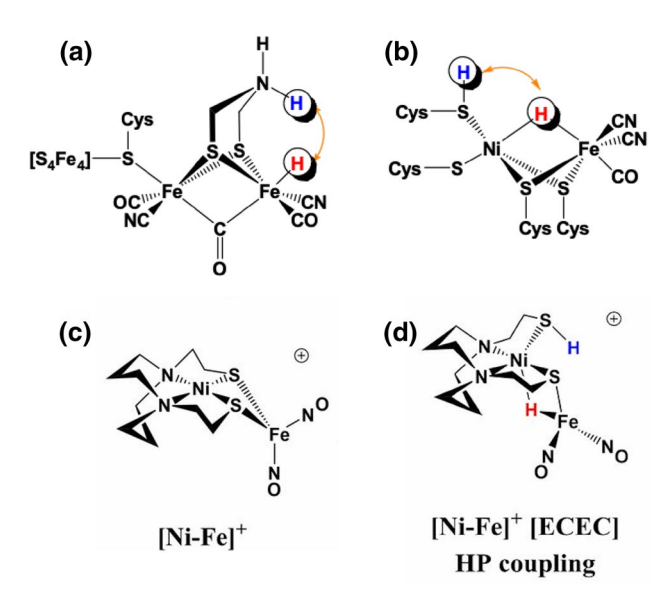


Fig. 1 a The active site of an [FeFe]- H_2 ase. **b** The active site of a [NiFe] H_2 ase. **c** A Ni-{Fe(NO)₂}⁹ bimetallic complex, previously reported to be a proton reduction catalyst. **d** A proposed catalytic intermediate in which the dissociated thiolate functions as a pendant base to position a proton near the metal hydride

bridging the Ni and Fe; it provides support for the basicity of nickel-bound thiolates [3].

While biomimetic studies of the tetra-cysteinate nickel binding site of [NiFe]-H₂ase are few, the utility of square planar NiN₂S₂ complexes as ligands to various transition metal ions has been widely reported for proton reduction electrocatalysis [4, 5]. Our laboratory has explored a set of Ni–Fe bimetallic complexes based on $[\eta^5-C_5H_5)Fe(CO)]^+$ and $\{Fe(NO)_2\}^{9/10}$ as receivers of the bidentate MN_2S_2 metallodithiolate ligands (Fig. 1c) [6]. According to trends and DFT computational results, induction of hemi-lability of MN₂S₂ through protonation at sulfur, or increased electron richness through reduction at the receiver metal site, or both, is key to the success of the electrocatalyst. As shown in Fig. 1d, the displacement of one arm of a protonated, nickel-bound thiolate from iron opens up a site for the generation of a hydride on iron. Thus, a well-positioned pendant base, needed for efficient proton-hydride coupling, is generated within the bimetallic by the hemi-lability of the nickel dithiolate.

A sequel to the above study began to address the scope of the ligand scaffold, detailing how the N_2S_2 ligand enabled proton reduction in MN_2S_2 -Fe' ($M=Ni^{II}$, [Fe(NO)]^{II}) complexes [7]. With the implication that a metal-bound thiolate is the precursor to the critical proton-binding site during catalytic turnover, we deemed it worthwhile to study the basicity of these nickel dithiolates in greater detail. In this report, we describe a method that utilizes UV–Vis spectroscopy to analyze the protonation of an NiN_2S_2 complex across numerous acid sources and apply this method to variously modified N_2S_2 ligands in order to examine structure/ function relationships.

Results and discussion

Correlation of N to N linkers and dithiolate bite angles in nickel-bound tetradentate N₂S₂ ligands

The metric parameters of NiN_2S_2 complexes based on diamines with ethanethiol arms reveal that the N to N carbon linker participates in a "clothespin" effect, i.e., constraints or pinching the nitrogens together widens the S-Ni-S angle [8]. Table 1 displays the NiN_2S_2 complexes examined in this study, along with pertinent metric data. Myriad synthetic applications of the NiN_2S_2 complexes as ligands to an exogenous metal or metals test chemists' intuition as this bite angle grants a significant bearing on the stability of the formed species. The NiN_2S_2 moiety can function as a bidentate metallodithiolate ligand in heterobimetallics, or



Table 1 Relevant bond angles and reduction potentials of nickel complexes examined in this report



Compound	Ni(bme-damp) [1Ni] [11]	Ni(bme-dame) [2Ni] [12]	Ni(bme-dach) [3Ni] [13]	Ni(bme-dachex) [4Ni] [14]	
N to N Carbon Linker	3	2	2, 3	2, 2	
N-N Distance (Å)	3.006(4)	2.698(6)	2.557(6)	2.392(3)	
S-S Distance (Å)	2.949(1)	3.173(2)	3.202(2)	3.343(2)	
S-Ni-S Angle	85.36(4)°	93.99(6)°	95.40(6)°	101.14(3)°	
Ni^{2+}/Ni^{+} (E _{pc} , V vs Fc ^{0/+}) ^a	-2.40 [15]	-2.32 [16]	-2.43 [15]	-2.35 [14]	

^aReduction potentials are reported as $E_{\rm nc}$ from acetonitrile [Bu₄N][PF₆] electrolyte solutions at 200 mV/s

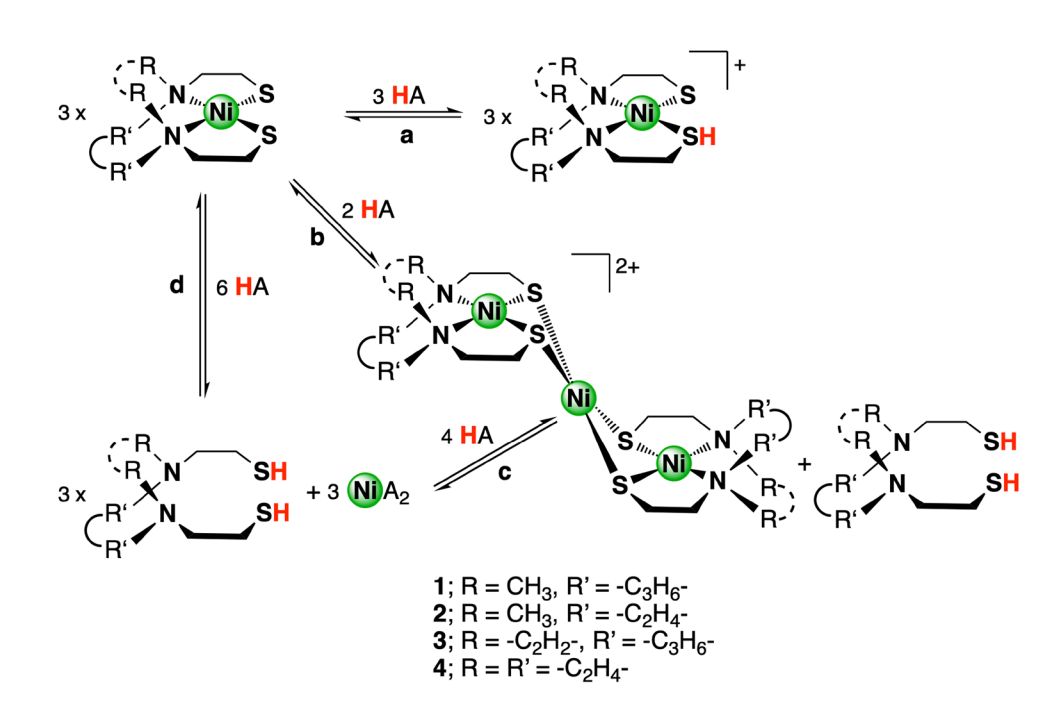
as a bidentate bridging ligand in the formation of multimetallic, paddlewheel complexes [9]. Early studies based on the bismercaptoethane-diazacyclooctane ligand, bmedaco, were plagued by a "thermodynamic sink", a prevalent tri-nickel species, [(bme-daco)Ni]₂Ni²⁺, that crystallized in a stair-step conformation [10]. Analogues of this tri-nickel species are common to most NiN₂S₂ complexes and serve as an analytical tool in this study. In the presence of certain acids, monomeric compounds [1Ni], [2Ni], and [3Ni] readily convert into the stair-step trimetallics, the crystal parameters of which are in the Cambridge Data Base. However, the NiN₂S₂ with the largest bite angle, [4Ni], has not been reported to form a trinuclear species and the data provided

herein suggest that such a species does not form under any conditions that were sufficient for the smaller angle species. The analytical procedure involved addition of acids of varying pK_a to the monomeric NiN_2S_2 species to bracket the pK_a of the dithiolate. The electronic spectral changes were interpreted according to the reaction equilibria given in Scheme 1.

Equilibrium between Ni(bme-dach) [3Ni] and strong acids

A methanol solution of Ni(bme-dach) (compound [3Ni], Scheme 1) features a d-d absorption band at 457 nm

 $\begin{array}{l} \text{Scheme 1} \quad \text{The four equilibria} \\ \text{observed between NiN}_2S_2 \text{ complexes } 1\text{--}4 \text{ and acids of varying } \\ \text{pK}_a \text{ values} \end{array}$





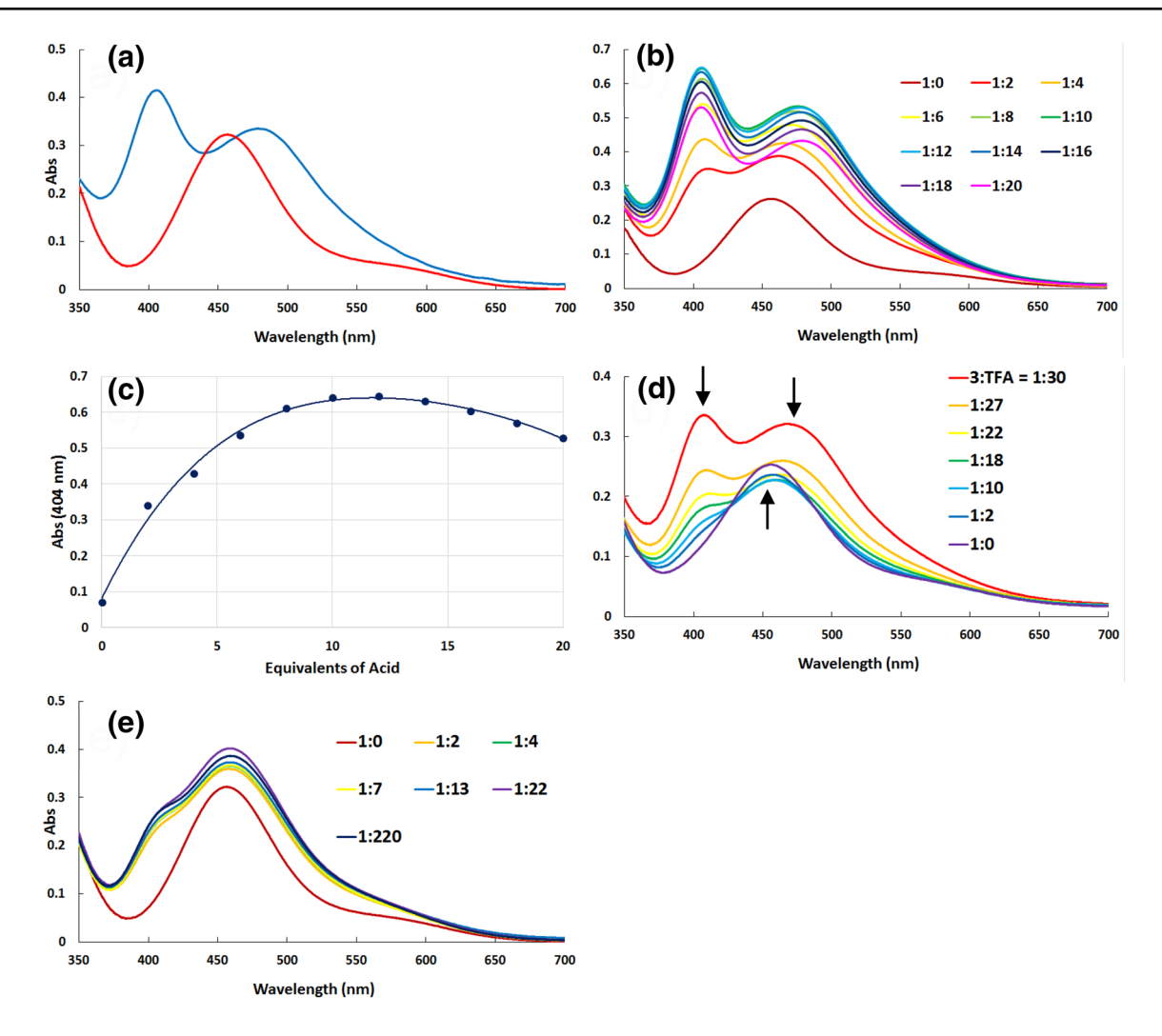


Fig. 2 a UV–Vis traces of 2.2 mM solution of [3Ni] (red) and 0.35 mM solution of $[3_2Ni_3]^{2+}$ (blue) in methanol. **b** Conversion of [3Ni] to $[3_2Ni_3]^{2+}$ by addition of several equivalents of trifluoroacetic acid (TFA). When the number of equivalents of TFA exceeds 12, the signal decreases, indicating the decomposition of $[3_2Ni_3]^{2+}$. **c** A plot of the absorbance at 404 nm, which correlates to $[3_2Ni_3]^{2+}$, versus equivalents of TFA. **d** UV–Vis traces of $[3_2Ni_3]^{2+}$ generated

from a 1:30 ratio of [3Ni] to TFA in methanol neutralized with aliquots of 5.3 M NaOH_(aq), regenerating [3Ni]. The inset legend reports the molar ratio of initial [3Ni] to unneutralized TFA. e Addition of phosphoric acid (H_3PO_4) to a solution of [3Ni] in methanol, showing the formation of a new species, assigned as the singly protonated $H[3Ni]^+$

with a molar extinction coefficient $\varepsilon_{457} = 558~{\rm M}^{-1}~{\rm cm}^{-1}$ (Fig. 2a). Upon addition of trifluoroacetic acid (TFA, pK_a=4.7 in MeOH) to the solution at ambient temperatures (~22 °C), peaks at 404 nm and 478 nm grow with greater molar absorptivity coefficients, $\varepsilon_{404} = 1950~{\rm M}^{-1}~{\rm cm}^{-1}$ and $\varepsilon_{478} = 1500~{\rm M}^{-1}~{\rm cm}^{-1}$, corresponding to the trimetallic species [Ni₃(bme-dach)₂]²⁺ ([3₂Ni₃]²⁺, Fig. 2b) [17]. An excess of acid is required to form [3₂Ni₃]²⁺, but too great an excess of TFA results in the decomposition of [3₂Ni₃]²⁺ and bleaching of the solution (Fig. 2c).

The requirement for excess acid suggests that the reaction exists as an equilibrium under these conditions. To test the reversibility of the [3Ni] to $[3_2Ni_3]^{2+}$ transformation, $[3_2Ni_3]^{2+}$ was generated with TFA in methanol solution followed by

the addition of aliquots of 5.3 M KOH_(aq). Addition of KOH regenerated the UV–Vis spectrum of 3 (Fig. 2d). Furthermore, on titration of independently synthesized $[3_2Ni_3]^{2+}$ (in the form of $[Ni_3(bme-dach)_2]Br_2$) with deprotonated bme-dach (Na₂bme-dach), the spectrum of [3Ni] was cleanly regained upon addition of one equivalent. With these data, we conclude that protonation of the thiolates of [3Ni] induce dissociation of the ligand to form $[3_2Ni_3]^{2+}$ and free H₂bme-dach. Deprotonation of the free ligand induces the central Ni²⁺ to reenter the N₂S₂ ligand tetradentate pocket, generating a clean solution of [3Ni].



Equilibrium between Ni(bme-dach) [3Ni] and weak acids

Titration of [3Ni] with weaker acids indicates the formation of a different product. As an aqueous solution of H_3PO_4 was added to a methanol solution of [3Ni], a shoulder grew in at 416 nm (Fig. 2e). As greater excesses of H_3PO_4 were added (> 200), the absorption at 416 nm saturated, i.e., the equilibrium was pushed to an effective quantitative yield of product. The trace of this product, however, is completely distinct from the trace of the trinuclear species. From these data, we propose that the equilibrium between [3Ni] and H_3PO_4 is not to form the trinuclear species, but rather a singly protonated species (Equilibrium a, Scheme 1). This fits the observations that this species is only observed with weaker acids but still participates in an equilibrium that can be saturated at high acid concentrations.

Examining equilibria with various acids

Determination of K_{eq} values for the equilibria in Scheme 1 was attempted using the percent conversion of monometallic to trimetallic species after each aliquot of acid was added. However, the complexity of co-existing equilibria, as well as the complete overlap of the product bands obscuring any isosbestic point, prevented consistent results. As an alternative approach to analyzing the nature of the equilibria, [3Ni] was titrated using an array of acids with varying pK_a values (Table 2). Acids with methanol-pK_a values < 5.44 participate in equilibrium **b**, forming $[3_2Ni_3]^{2+}$ as a product and, upon further addition, decompose [3₂Ni₃]²⁺ (equilibrium c, Scheme 1). Dichloroacetic acid (MeOH $pK_a = 6.38$) and pyridinium p-toluenesulfonate (PPTS, MeOH p K_a = 5.44) participate in Equilibrium **b**, but do not decompose the product as more acid is added. Acids with methanol-pK_a values above 6.38 but below 10.9 participate in equilibrium a, forming H[3Ni]⁺. Acids with methanol $pK_a \ge 14.3$ do not react with [3Ni] at any concentration.

Table 2 Reactivity of nickel complexes ligated by **1–4** with an array of acids in methanol. Equilibria observed correlate with those describe in Scheme 1. The more flexible ligands (1 and 2) show the tendency to form the tri-nickel species even with weaker acids. The

When these equilibria were examined in aqueous solution, no change to [3Ni] was observed, regardless of the acid used.

Equilibrium with Ni(bme-dame) [2Ni]

The Ni(bme-dame) complex ([2Ni], Table 1) has also been shown to form a trimetallic species, $[Ni_3(bme-dame)_2]^{2+}$ (compound $[2_2Ni_3]^{2+})[21]$, thus offering opportunity to extend our analytical method to explore the ligand effect on the observed equilibrium.

Addition of TFA to a methanol solution of [2Ni] generates peaks at 416 nm and 480 nm in a manner reminiscent of the transformation observed with [3Ni] (Fig. 3a). Also similar to the equilibrium with [3Ni], as a greater excess of TFA is added, [2₂Ni₃]²⁺ decomposes and the solution begins to bleach. Compound [2Ni] was titrated with an array of acids to determine which acids participate in which equilibria (Table 2). No evidence was found for equilibrium a, but equilibria b and c were observed (Scheme 1).

In comparison to [3Ni], [2Ni] forms the tri-nickel species with fewer equivalents of acid and with acids of greater pK_a . We posit that the increased flexibility of the bme-dame ligand allows for easier dissociation of the ligand from the nickel; thus, weaker acids are more prone to form the trimetallic species over the mono-protonated species.

Equilibrium with Ni-bme-damp [1Ni]

The trimetallic form of Ni(bme-damp) (complex [1Ni], Table 1) was isolated and characterized by XRD as the typical stair-step configuration (Fig. 4). The S–Ni–S angle within the $\rm N_2S_2$ binding site is 79.97(9)°, a 5.39° contraction from the angle of the mononuclear species, 85.36(4)°. This is coupled with a decrease of the S–S distance from 2.949(1) to 2.791(2). The N–N distance, however, remains at 3.009(7) Å, which is within error of the mononuclear N–N distance, 3.006(4) Å. The stair-step angle is 76.55°.

more rigid 3 has the capacity to bind a single proton from weaker acids without forming the tri-nickel species. The most strained ligand, 4, readily releases the nickel from the N_2S_2 pocket upon protonation, but is incapable of forming the tri-nickel species [18–20]

pK _a (in H ₂ O)	HBF ₄	CF ₃ CO ₂ H	CCl ₃ CO ₂ H	PPTS	CHCl ₂ CO ₂ H	H ₃ PO ₄	CH ₃ CO ₂ H	NH ₄ Cl	PhOH	CF ₃ CH ₂ OH
	-0.44	-0.25	0.65	5.21	1.29	2.12	4.76	9.24	9.95	12.5
pK _a (in MeOH)	_	4.7 ^a	5.6 ^a	5.44	6.38	5.2 ^b	9.63	10.9	14.3	_
Ni(bme-damp) [1Ni]	b, c	b, c	b, c	b, c	b, c	b, c	b	b	b	NR
Ni(bme-dame) [2Ni]	b, c	b, c	b, c	b, c	b, c	b, c	b	b	NR	NR
Ni(bme-dach) [3Ni]	b, c	b, c	b, c	b	b	a	a	a	NR	NR
Ni(bmedach _{ex}) [4Ni]	d	d	d	d	d	d	d	NR	NR	NR

^aValues calculated from linear correlation of carboxylic acids in methanol [19]



^bValue determined from interpolation of methanol/water mixtures [20]

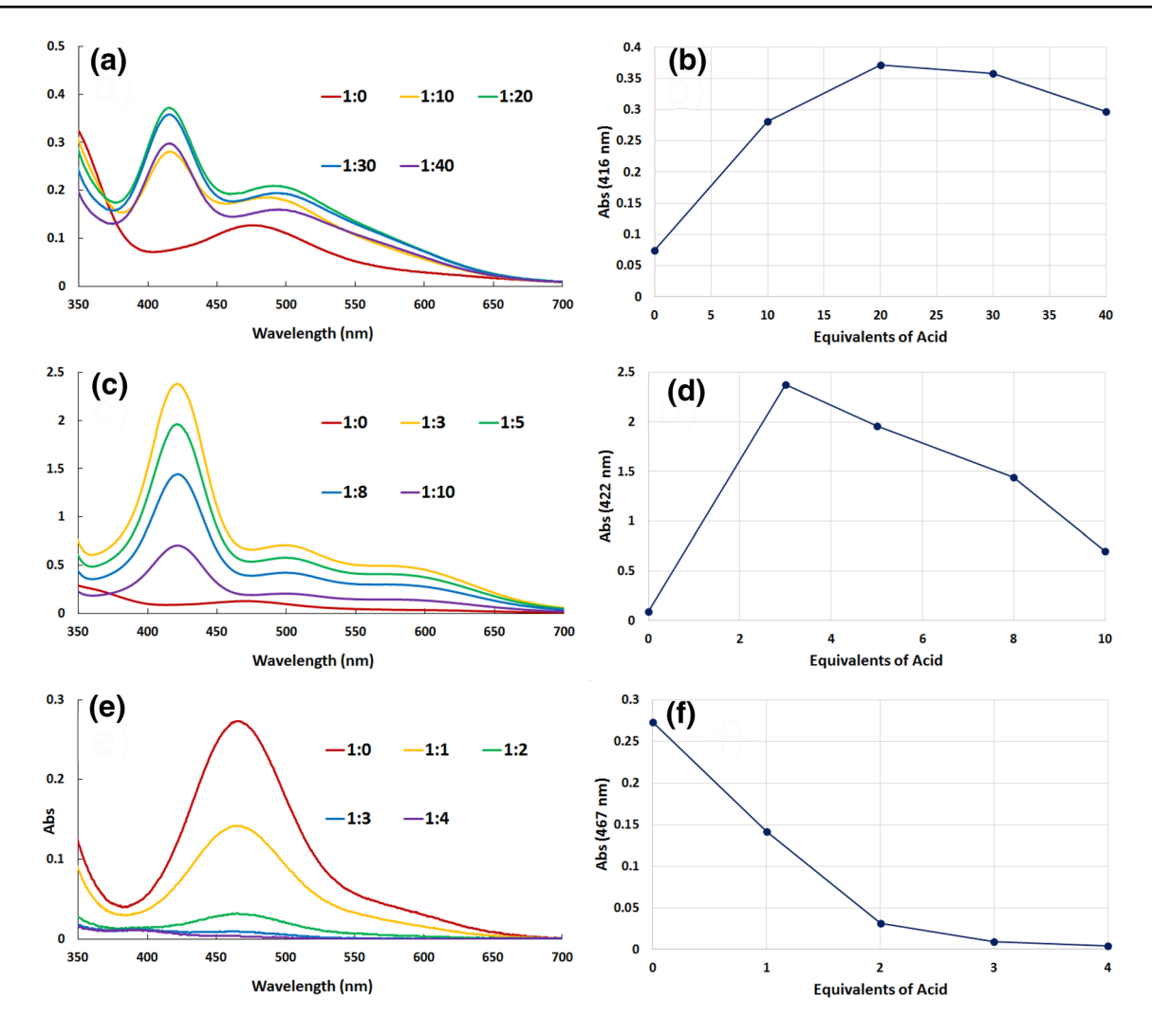
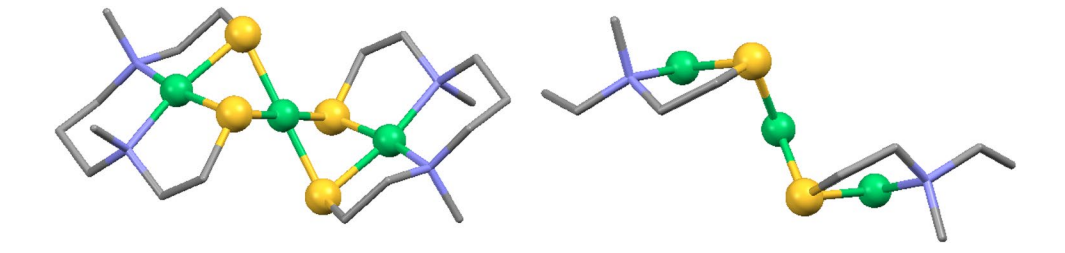


Fig. 3 a UV–Vis traces of methanol solution of [2Ni] with decreasing ratios of [2Ni] to TFA. b The absorbance of 416 nm, which correlates to $[2_2Ni_3]^{2+}$ versus equivalents of TFA. c UV–Vis traces of methanol solution of [1Ni] with decreasing ratios of [1Ni] to TFA.

d The absorbance of 422 nm, which correlates to $[1_2Ni_3]^{2+}$ versus equivalents of TFA. **e** UV–Vis traces of methanol solution of **[4Ni]** with decreasing ratios of **[4Ni]** to TFA. **f** The absorbance of 467 nm, which correlates to **[4Ni]** versus equivalents of TFA

Fig. 4 Two views of the XRD-determined structure of $[1_2Ni_3]^{2+}$. Nickel atoms shown in green, sulfur atoms in yellow, nitrogen atoms blue, and carbon atoms in gray



The equilibrium of [1Ni] with the array of acids was examined to probe how further flexibility of the ligand would affect reactivity (Table 2). Similar to compounds [2Ni] and [3Ni], addition of TFA to a methanol solution of [1Ni] causes the appearance of a two-peak pattern, with a stronger band at 422 nm and a weaker band around 500 nm, that bleaches upon greater excess of acid (Fig. 3c).

The reactivity of [1Ni] appears to be most similar to that of [2Ni], with the trimetallic complex forming readily even with weaker acids. The most notable difference is that [1Ni] reacts with an excess of phenol, but it is difficult to conclude whether [1Ni] converts to $[1_2Ni_3]^{2+}$ or a mono-protonated species. Compounds [2Ni] and [1Ni] with open-chain N to



N connections show an appreciable increase in susceptibility to ligand dissociation as compared to the diazacyclic [3Ni].

Equilibrium with Ni(bme-dachex) [4 Ni]

In contrast to the more flexible N to N connections found in complexes 1 and 2, the Ni-bmedachex ([4Ni], Table 1) complex features a cyclohexyl-diazacycle platform which reduces flexibility of the ligand and substantially increases the S-Ni-S angle compared to [3Ni] [14]. Addition of TFA to a methanol solution of [4Ni] yielded spectral results very different from the other compounds of this study. Rather than generating a new product with greater absorptivity coefficients, it simply bleached the solution, causing the d-d band to decrease in intensity (Fig. 3e). This same result was observed with weaker acids down to acetic acid (Table 2).

The tri-nickel species with bme-dachex has not been described previously in the literature [8]. The only example of the binding of Ni(bme-dachex) to an exogenous nickel center comes from the Schröder group who describe a Ni(bme-dachex) pinwheel type complex, Ni₂(Ni(bme-dachex))₄⁴⁺, in which the S to S distance of one binucleating Ni(bme-dachex) ligand maintains its wide S-Ni-S angle [22]. The paddlewheel compound of the Schröder group is described as being dark red in color, so it is unlikely that it is formed as the acids are added to [4Ni]. Instead, the data are most consistent with the hypothesis that the acids cause dissociation of the ligand from the nickel center to generate free bme-dachex and the nickel conjugate base salt (equilibrium d, Scheme 1).

There is no indication of an intermediate $H[4Ni]^+$ species when [4Ni] is mixed with ammonium chloride, as was seen with [3Ni], suggesting that [3Ni] is at least slightly more basic than [4Ni]. This, however, is somewhat disputed by the fact that acetic acid does not induce dissociation of the ligand from [3Ni] as it does for [4Ni]. The model most consistent with these data is that the bme-dach ligand does not dissociate from the nickel after a single protonation, and thus $H[3Ni]^+$ is observed, but the hypothetical $H[4Ni]^+$

intermediate rapidly degrades to the free ligand and nickel salt.

Electrochemical studies

The complexes examined in this study have been previously characterized by cyclic voltammetry in acetonitrile solutions and all feature reduction of the nickel(II) at potentials <-2.3 V vs Fc^{0/+} (Table 1) [14–16]. In the case of [2Ni], the complex was found to reduce protons to form hydrogen electrocatalytically [16]. Although the Ni^{2+/+} reductions are outside the solvent window of methanol, the four complexes were studied via cyclic voltammetry in methanol solution in the presence and absence of acetic acid.

The initial scan of [3Ni] from the open circuit potential in the cathodic direction and in the absence of acid features no reduction event, but an irreversible oxidation with $E_{\rm pa} = 0.04 \text{ V vs Fc}^{0/+}$ at 200 mV/s (Fig. 5a). The return sweep finds that oxidation induces an irreversible reduction event with an $E_{\rm pc} = -1.18$ V vs Fc^{0/+} at 200 mV/s. These events are described as the oxidation, and subsequent reduction, of the sulfur atoms. When acetic acid is added to the solution, which participates in equilibrium a with [3Ni] (Table 2), the reduction of acetic acid itself can be observed at the same potential as a control experiment in the absence of Ni²⁺. The oxidation event of 3 shifts slightly more positive to $E_{\rm pa} = 0.01 \text{ V}$ vs Fc^{0/+} at 200 mV/s in the presence of acidic acid (Fig. 5b), but the reduction event shifts significantly to $E_{\rm nc} = -1.28$ V vs Fc^{0/+} at 200 mV/s. The shifts in potentials of these sulfur-based redox events could be the result of proton binding to the sulfur sites in solution.

The cyclic voltammograms of [1Ni], [2Ni], and [4Ni] show similar features. Compound 2 displays an irreversible oxidation with $E_{\rm pa}$ =0.01 V vs Fc^{0/+} at 200 mV/s that does not shift significantly in the presence of acid and the corresponding irreversible reduction event at $E_{\rm pc}$ =-1.13 V vs Fc^{0/+} at 200 mV/s that shifts to -1.15 V in upon addition of acetic acid (Figure S8). Compound 1 shows an irreversible oxidation with $E_{\rm pa}$ =0.01 V vs Fc^{0/+} at 200 mV/s that shifts to 0.02 V with

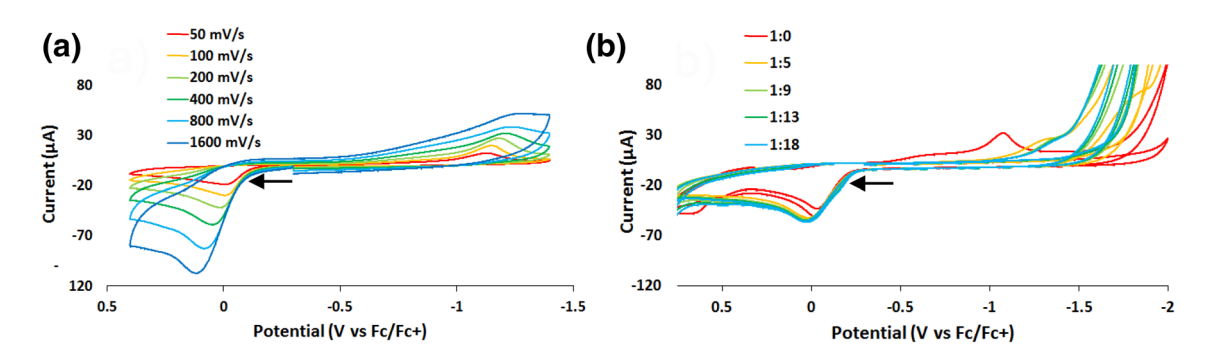


Fig. 5 a Cyclic voltammogram (CV) of [3Ni] in MeOH with 0.1 M $[Bu_4N][PF_6]$ electrolyte at various scan rates. b CV of [3Ni] with increasing ratios of acetic acid in solution with 200 mV/s scan rate



acetic acid, but only a faintly visible irreversible reduction at $\sim -1.0~\rm V~vs~Fc^{0/+}$ (Figure S7). Compound [4Ni] features two irreversible oxidations with $E_{\rm pa}\!=\!0.02~\rm V$ and 0.39 V vs Fc^0/+ at 200 mV/s, the more positive of which induces an irreversible reduction at -1.58 V (Figure S9). In the presence of acetic acid, the more positive reduction shifts to 0.47 V vs Fc^0/+ at 200 mV/s, but the reduction event becomes obscured by the reduction of the acid. The shift of the $E_{\rm pa}$ by +0.08 V could be the result of the formation of free protonated ligand being generated in the solution.

Conclusions

The results presented in this manuscript reveal the effects of ligand flexibility on the behavior of N₂S₂ ligand thiolates upon protonation. Even in the presence of mild acids such as phenol and ammonium, highly flexible ligands such as bmedamp and bme-dame readily release a nickel from its N₂S₂ pocket, subsequently rapidly scavenging unprotonated NiN₂S₂ to form the trimetallic complex. The more constrained ligand of optimal geometric parameters, the diazacycle bme-dach, is capable of maintaining coordination to the nickel center after single protonation from modest acids (phosphoric and acetic acids), but will also form a trimetallic complex upon protonation with stronger acids (pyridinium). If the ligand is very constrained, as is the case with cyclohexyl-diazacycle bmedachex, the ligand will readily dissociate from the nickel center upon protonation by any acid of sufficient strength to protonate it at all. These findings highlight the importance of ligand structure when utilizing metalloligands as pendent bases for catalysis. Even modest adjustments can yield significant variations to the reactivity, basicity, and stability of the complex upon protonation.

Acknowledgements This manuscript is submitted in recognition and appreciation of the bioinorganic research of Joan Broderick that has so greatly advanced understanding of the critical roles of iron-sulfur chemistry within biosynthetic pathways. Our work was funded by the National Science Foundation (CHE-1665258) and the Robert A. Welch Foundation (A-0924).

Compliance with ethical standards

Conflict of interest The authors declare no conflict of interest.

Data availability The crystallographic data for complex were deposited in the Cambridge Crystallographic Data Centre with a CDC number 1917616.

References

 Lubitz W, Ogata H, Rüdiger O, Reijerse E (2014) Hydrogenases. Chem Rev 114:4081–4148

- Schilter D, Camara JM, Huynh MT, Hammes-Schiffer S, Rauchfuss TB (2016) Hydrogenase enzymes and their synthetic models: the role of metal hydrides. Chem Rev 116:8693–8749
- Yagi T, Ogo S, Higuchi Y (2014) Catalytic cycle of cyctochromec3 hydrogenase, a [NiFe]-enzyme, deduced from the structures of the enzyme and the enzyme mimic. J Hydrogen Energ 39:18543–18550
- Ogo S, Ichikawa A, Kishima T, Matsumoto T, Nakai H, Kusaka K, Ohhara T (2013) A functional [NiFe]hydrogenase mimic that catalyzes electron and hydride transfer from H₂. Science 339:682–684
- Canaguier S, Field M, Oudart Y, Pecaut J, Fontecave M, Artero V (2010) A structural and functional mimic of the active sire of NiFe hydrogenase. Chem Commun 46:5876–5878
- Ding S, Ghosh P, Darensbourg MY, Hall MB (2017) Interplay of hemilability and redox activity in models of hydrogenase active sites. Proc Natl Acad Sci USA 114(46):E9775–E9782
- Ghosh P, Ding S, Chupik RB, Quiroz M, Hsieh C, Bhuvanesh N, Hall MB, Darensbourg MY (2017) A matrix of heterobimetallic complexes for interrogation of hydrogen evolution reaction electrocatalysts. Chem Sci 8:8291–8300
- Stibrany RT, Fox S, Bharadwaj PK, Schugar HJ, Potenza JA (2005) Structural and spectroscopic features of mono- and binuclear nickel(II) complexes with tetradentate N(amine)₂S(thiolate)₂ ligation. Inorg Chem 44:8234–8242
- Denny JA, Darensbourg MY (2015) Metallodithiolates as ligands in coordination, bioinorganic, and organometallic chemistry. Chem Rev 115:5248–5273
- Farmer PJ, Solouki T, Mills DK, Soma T, Russell DH, Reibenspies JH, Darensbourg MY (1992) Isotopic labeling investigation of the oxygenation of nickel-bound thiolates by molecular oxygen. J Am Chem Soc 114:4601–4605
- Colpas GJ, Kumar M, Day RO, Maroney MJ (1990) Structural investigations of nickel complexes with nitrogen and sulfur donor ligands. Inorg Chem 29:4779–4788
- Hosler ER, Herbst RW, Maroney MJ, Chohan BS (2012) Exhaustive oxidation of a nickel dithiolate complex: some mechanistic insights en route to sulfate formation. Dalton Trans 41:804–816
- Smee JJ, Miller ML, Grapperhaus CA, Reibenspies JH, Darensbourg MY (2001) Subtle bite-angle influences on N₂S₂Ni complexes. Inorg Chem 40:3601–3605
- Zhao T, Ghosh P, Martinez Z, Liu X, Meng X, Darensbourg MY (2017) Discrete air-stable nickel(II)-palladium(II) complexes as catalysts for Suzuki-Miyaura reactions. Organometallics 36:1822–1827
- Rampersad MV, Jeffery SP, Golden ML, Lee J, Reibenspies JH, Darensbourg DJ, Darensbourg MY (2005) Characterization of steric and electronic properties of NiN₂S₂ complexes as S-donor metallodithiolate ligands. J Am Chem Soc 127:17323–17334
- Luo G, Wang Y, Wang J, Wu J, Wu R (2017) A Square-planar nickel dithiolate complex as an efficient molecular catalyst for the electro- and photoreduction of protons. Chem Commun 53:7007-7010
- Golden ML, Jeffrey SP, Miller ML, Reibenspies JH (2004) Darensbourg MY (2004) The construction of (N₂S₂)Ni-Pd clusters: a slant-chair, a basket and a C4-paddlewheel structure. Eur J Inorg Chem 2:231–236
- 18. Evans D, Ripin DH (2005) Evans pKa Table. Web Resource, p 1–6
- Rived F, Marti Roses, Bosch E (1998) Dissociation constants of neutral and charged acids in methyl alcohol. The acid strength resolution. Anal Chim Acta 374:309–324
- Bhattacharyya A, Maandal AK, Lahiri SC (1980) Conductometric studies on the dissociation constants of phosphoric acid in methanol-water mixtures. Electrochim Acta 25:529–561
- Turner MA, Driessen WL, Reedijk J (1990) Synthesis, structure, and properties of a trinuclear and a mononuclear nickel(II)



- complex of N, N'-dimethyl-N, N'-bis(mercaptoethyl)ethylenediamine. Inorg Chem 29:3331–3335
- Amoroso AJ, Chung SSM, Spencer DJE, Danks JP, Glenny MW, Blake AJ, Cooke PA, Wilson C (2003) Schroder M (2003) Pinwheel motifs: formation of unusual homo- and hetero-nuclear aggregates via bridging thiolates. Chem Commun 16:2020–2021

Publisher's Note Springer Nature remains neutral with regard to jurisdictional claims in published maps and institutional affiliations.

Affiliations

Nicholas A. Arnet¹ · Nattamai Bhuvanesh¹ · Marcetta Y. Darensbourg¹

Marcetta Y. Darensbourg marcetta@chem.tamu.edu

Department of Chemistry, Texas A&M University, College Station, TX 77840, USA

